The azimuthal magnetorotational instability (AMRI)

G. Rüdiger[1,*], **R. Hollerbach**[2], **M. Gellert**[1], and **M. Schultz**[1]

[1] Astrophysikalisches Institut Potsdam, An der Sternwarte 16, D-14482 Potsdam, Germany
[2] Department of Applied Mathematics, University of Leeds, Leeds, LS2 9JT, United Kingdom

We consider the flow of an electrically conducting fluid between differentially rotating cylinders, in the presence of an externally imposed current-free toroidal field $B_0(R_{in}/R)\,\hat{e}_\phi$. It is known that the classical, axisymmetric magnetorotational instability does not exist for such a purely toroidal imposed field. We show here that a nonaxisymmetric magnetorotational instability does exist, having properties very similar to the axisymmetric magnetorotational instability in the presence of an axial field. In the nonlinear regime the magnetic energy of the perturbances is shifted (in the sense of an inverse cascade) to the axisymmetric mode rather than to the modes with $m > 1$.

1 Introduction

The magnetorotational instability (MRI) is a mechanism whereby a hydrodynamically stable differential rotation flow may be destabilized by the addition of a current-free magnetic field. The original view was that the axial component of the field is the only important one, with any azimuthal component playing no essential role, and incapable of producing any instabilities on its own (Velikhov 1959; Balbus & Hawley 1991). This view was altered by the discovery that a mixed axial and azimuthal field yields instabilities quite different in many ways from those found with a purely axial field (Hollerbach & Rüdiger 2005; Rüdiger et al. 2005). Here we show that even a purely azimuthal field yields an MRI, and compare its properties with the previously known types. Often the toroidal field amplitude exceeds the poloidal one by orders of magnitude so that it should be possible to ignore the influence of the latter. This is certainly not true if both components are of the same order (see Broderick & Narayan 2007). It might easily be that the MRI of an azimuthal field ("AMRI", see Rüdiger et al. 2007) plays a more important role in real astrophysical objects such like accretion disks with $B_{tor} \gg B_{pol}$ (see Ogilvie & Pringle 1996).

While its most important application is to astrophysical accretion disks (Balbus & Hawley 1991), the MRI was originally discovered in the much simpler Taylor-Couette problem, consisting of the flow between differentially rotating cylinders (Velikhov 1959). Because of its relative simplicity, this geometry has proven particularly amenable both to theoretical analyses of the MRI (Rüdiger & Zhang 2001; Ji, Goodman & Kageyama 2001), as well as to its recent experimental realization (Stefani et al. 2006; Rüdiger et al. 2006).

Consider therefore an electrically conducting fluid confined between two concentric cylinders of radii R_{in} and R_{out}, rotating at rates Ω_{in} and Ω_{out}, chosen to satisfy $\Omega_{out}R_{out}^2 > \Omega_{in}R_{in}^2$. That is, the angular momentum increases outward, so by the familiar Rayleigh criterion the flow is hydrodynamically stable, with the angular velocity given by

$$\Omega(R) = A + \frac{B}{R^2}, \tag{1}$$

where

$$A = \frac{\Omega_{out}R_{out}^2 - \Omega_{in}R_{in}^2}{R_{out}^2 - R_{in}^2}, \;\; B = \frac{R_{in}^2 R_{out}^2(\Omega_{in} - \Omega_{out})}{R_{out}^2 - R_{in}^2}. \tag{2}$$

Here we will fix $R_{out} = 2R_{in}$ and $\Omega_{out} = \Omega_{in}/2$, so A and B simplify to $\frac{1}{3}\Omega_{in}$ and $\frac{2}{3}\Omega_{in}R_{in}^2$, respectively. The essence of the MRI then is to ask whether the addition of a *force-free* magnetic field can destabilize this flow.

If the imposed field is purely axial, $\boldsymbol{B}_0 = B_0\,\hat{e}_z$, the profile (1) can be destabilized, provided the rotation rates are sufficiently great, and the field strength B_0 is neither too weak nor too strong. Specifically, the magnetic Reynolds number

$$\mathrm{Rm} = \frac{\Omega_{in}R_{in}^2}{\eta}, \tag{3}$$

where η is the magnetic diffusivity, must exceed $O(10)$, and the Lundquist number

$$\mathrm{S} = \frac{B_0 R_{in}}{\sqrt{\rho\mu}\,\eta}, \tag{4}$$

where ρ is the density and μ the permeability, must be around 3–10.

In contrast, if the imposed field is mixed axial and azimuthal,

$$\boldsymbol{B}_0 = B_0\,\hat{e}_z + \beta B_0(R_{in}/R)\,\hat{e}_\phi, \tag{5}$$

* Corresponding author: gruediger@aip.de

where β is around 1–10, then the profile (1) can again be destabilized, but at very different rotation rates and field strengths (Hollerbach & Rüdiger 2005). The relevant parameter measuring the rotation rates is now not the magnetic Reynolds number, but rather the hydrodynamic Reynolds number $\mathrm{Re} = \Omega_{\mathrm{in}} R_{\mathrm{in}}^2/\nu$, where ν is the viscosity. Similarly, the parameter measuring the field strength is not the Lundquist number, but instead the Hartmann number $\mathrm{Ha} = B_0 R_{\mathrm{in}}/\sqrt{\rho\mu\eta\nu}$. The MRI sets in when $\mathrm{Re} \gtrsim O(10^3)$, and $\mathrm{Ha} \approx O(10)$.

To compare these results, we note that the two sets of parameters are related by $\mathrm{Re} = \mathrm{Rm}\,\mathrm{Pm}^{-1}$ and $\mathrm{Ha} = \mathrm{S}\,\mathrm{Pm}^{-1/2}$, where

$$\mathrm{Pm} = \frac{\nu}{\eta} \qquad (6)$$

is the magnetic Prandtl number. Typical values for liquid metals (gallium) are $O(10^{-6})$. Translating the results for the purely axial field, we thus obtain $\mathrm{Re} \gtrsim O(10^7)$ and $\mathrm{Ha} \approx O(10^4)$, both several orders of magnitude greater than for the mixed field. It is perhaps not surprising then that the MRI has been obtained experimentally for the mixed field (Stefani et al. 2006; Rüdiger et al. 2006), but not (yet) for the purely axial field.

Nonaxisymmetric modes have also been explored, for both the purely axial as well as the mixed fields. For a purely axial field the relevant parameters are still Rm and S, but the critical values Rm_c are larger than for the axisymmetric modes, indicating that the axisymmetric MRI is the most unstable mode. For mixed fields, one finds – perhaps somewhat surprisingly – that adding an azimuthal component now has minimal effect, certainly far less than the reduction by four orders of magnitude found for the axisymmetric modes. Evidently the relevant parameters continue to be Rm and S, rather than Re and Ha.

2 Marginal instability

We shall show that for these nonaxisymmetric modes, one can impose a purely azimuthal field, $B_0(R_{\mathrm{in}}/R)\,\hat{\mathbf{e}}_\phi$, and still obtain an MRI, having all the characteristics of the previous nonaxisymmetric types of MRI. To this end, we solve the linear stability equations

$$\mathrm{Rm}\,\frac{\partial \boldsymbol{b}}{\partial t} = \mathrm{rot}(\boldsymbol{u} \times \boldsymbol{B}_0) + \mathrm{Rm}\,\mathrm{rot}(\boldsymbol{U}_0 \times \boldsymbol{b}) + \Delta\boldsymbol{b}, \qquad (7)$$

$$\mathrm{Re}\,\frac{\partial \boldsymbol{u}}{\partial t} = -\nabla p + \mathrm{Ha}^2\,\mathrm{rot}\boldsymbol{b} \times \boldsymbol{B}_0 +$$
$$+ \mathrm{Re}\,(\boldsymbol{U}_0 \times \mathrm{rot}\boldsymbol{u} + \boldsymbol{u} \times \mathrm{rot}\boldsymbol{U}_0) + \Delta\boldsymbol{u}, \qquad (8)$$

where $\boldsymbol{U}_0 = R\Omega(R)\,\hat{\mathbf{e}}_\phi$ is the profile (1) whose stability we are exploring, and $\boldsymbol{B}_0 = B_0(R_{\mathrm{in}}/R)\,\hat{\mathbf{e}}_\phi$ is the imposed current-free azimuthal field. Its current everywhere vanishes except along the vertical axis which does not belong to our computational domain. Length has been scaled by R_{in}, time by $\Omega_{\mathrm{in}}^{-1}$, $\boldsymbol{U}_0$ and $\boldsymbol{u}$ as $R_{\mathrm{in}}\Omega_{\mathrm{in}}$, $\boldsymbol{B}_0$ as B_0, and $\boldsymbol{b}$ as $\mathrm{Rm}B_0$.

Taking the t, z and ϕ dependence to be of the form $\exp(\omega t + \mathrm{i}kz + \mathrm{i}m\phi)$, and using also $\mathrm{div}\,\boldsymbol{b} = 0$ to eliminate b_z, the r and ϕ components of Eq. (7) become

$$\mathrm{Rm}\,\omega b_R = \Delta b_R - R^{-2}b_R - 2\mathrm{i}mR^{-2}b_\phi + \mathrm{i}mR^{-2}u_R -$$
$$- \mathrm{Rm}\,\mathrm{i}m\Omega\,b_R, \qquad (9)$$

$$\mathrm{Rm}\,\omega b_\phi = \Delta b_\phi - R^{-2}b_\phi + 2\mathrm{i}mR^{-2}b_R + \mathrm{i}mR^{-2}u_\phi +$$
$$+ 2R^{-2}u_R - \mathrm{Rm}\,\mathrm{i}m\Omega\,b_\phi + \mathrm{Rm}\,Rb_R\,\mathrm{d}\Omega/\mathrm{d}R. \qquad (10)$$

The components of Eq. (8) have a similar structure. The boundary conditions are

$$b_R = \mathrm{d}b_\phi/\mathrm{d}R + R^{-1}b_\phi = u_R = u_\phi = u_z = 0 \qquad (11)$$

at $R = R_{\mathrm{in}}$ and R_{out}, corresponding to perfectly conducting, no-slip walls. The resulting 1D linear eigenvalue problem is solved by finite differencing in R.

Figure 1 shows the stability curves for $m = 1$, the only mode that appears to become unstable. We see how an MRI exists that is remarkably similar to some of the results described above. In particular, as $\mathrm{Pm} \to 0$, the relevant parameters are clearly once again Rm and S, with the MRI arising if $\mathrm{Rm} \gtrsim 80$, and $\mathrm{S} \approx 40$. The specific numbers are roughly an order of magnitude greater than for the axisymmetric MRI in the axial field, but the basic scalings, and even the shape of the instability curves, are identical.

One basic difference, however, can be observed. For each magnetic Prandtl number Pm there is a minimum Lundquist number S which must be exceeded for instability. Modes with $m = 1$ do not appear for $\mathrm{Rm} \to \infty$ if $\mathrm{S} \to 0$. In other words, for given S there is a minimum Rm, and a maximum Rm between the instability exists. This is a direct consequence of the fact that nonaxisymmetric (here $m = 1$) instabilities are stabilized by strong differential rotation.

From Fig. 1 one obtains the simple relation $\mathrm{Rm} \simeq 2\mathrm{S}$ for the minimum values, valid for Pm varying over 3 orders of magnitudes. Hence, we find for the linear velocity of the inner cylinder

$$u_{\mathrm{in}} \simeq 2V_{\mathrm{A}}, \qquad (12)$$

with V_{A} as the Alfvén velocity of the toroidal field B_{in}. For $\mathrm{Pm} > 1$ one can see that $\mathrm{S}_{\mathrm{crit}} \propto \sqrt{\mathrm{Pm}}$, so that $B_{\mathrm{crit}} \propto \sqrt{\nu\eta}$ for $\nu \gg \eta$. Similarly, $\Omega_{\mathrm{in}} \propto \sqrt{\nu\eta}$. However, if the viscosity is small ($\nu \ll \eta$) it does not play any role.

For sufficiently high S one finds instability if the rotation is neither too slow nor too fast: $V_{\mathrm{A}} < u_{\mathrm{in}} < 4V_{\mathrm{A}}$. But also: for sufficiently high Rm the magnetic field must not be neither too weak nor too strong.

Figure 2 shows the real part of ω in the unstable regime. Remembering that time has been scaled by $\Omega_{\mathrm{in}}^{-1}$, we see that we obtain growth rates as large as $0.05\Omega_{\mathrm{in}}$. So again, while the particular number 0.05 is about an order of magnitude smaller than for the axisymmetric MRI in the axial field, this nonaxisymmetric AMRI is clearly also growing on the basic rotational timescale. Note that the growth rate increases for decreasing magnetic Prandtl number. If the viscosity is high ($\nu \gg \eta$) the azimuthal magnetorotational instability is thus *stabilized*.
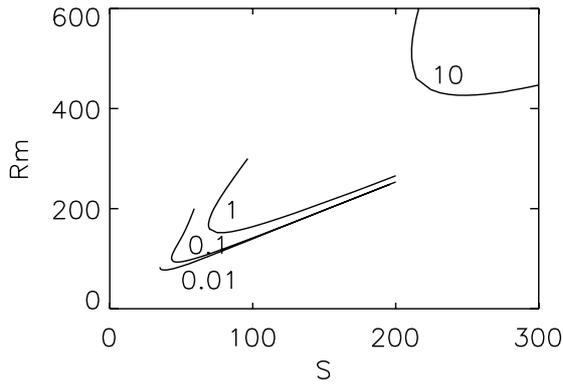
Fig. 1   The critical magnetic Reynolds number Rm for the onset of AMRI, as a function of the Lundquist number S, for different values of Pm. $m = 1$, $R_{out}/R_{in} = 2$, $\Omega_{out}/\Omega_{in} = 0.5$.
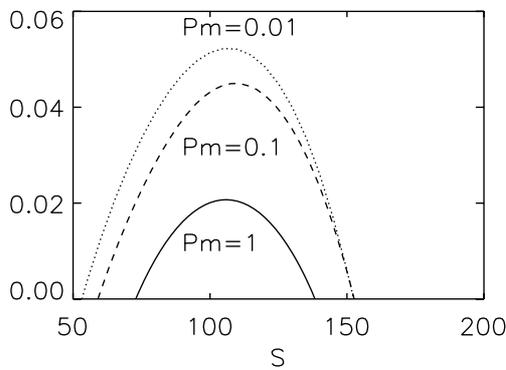

Fig. 2   The growth rate of the AMRI normalized with Ω_{in} as functions of S for Rm $= 200$ for various magnetic Prandtl numbers Pm.

Fig. 3   The marginally stable solution at Pm $= 0.1$, S $= 47.4$ and Rm $= 93$ (see Fig. 1). From left to right the R, ϕ and z components of $\boldsymbol{u}$ (*top*) and $\boldsymbol{b}$ (*bottom*). The real parts are solid, imaginary parts dashed. Note how both $\boldsymbol{u}$ and $\boldsymbol{b}$ have the z components largest. The azimuthal wavenumber is $k = 1.88$.

To understand why this nonaxisymmetric MRI exists even for a purely toroidal field $\boldsymbol{B}_0$, for which it is known that the axisymmetric MRI fails, we need to consider the details of Eqs. (9) and (10). In particular, note that for $m = 0$, b_R completely decouples from everything else, and inevitably decays away. Without b_R though, the MRI cannot proceed, as it relies on the term Rm $\Omega' R b_R$ in Eq. (10). In contrast, for $m = 1$, b_R is coupled both to b_ϕ, coming from $\Delta\boldsymbol{b}$, and to u_R, from rot($\boldsymbol{u} \times \boldsymbol{B}_0$). And once b_R is coupled to the rest of the problem, the term Rm $\Omega' R b_R$ then allows the AMRI to develop. Figure 3 presents an example of these solutions, indicating how all three components of both $\boldsymbol{u}$ and $\boldsymbol{b}$ are indeed present. The plots also show that AMRI is not a boundary layer phenomenon.

3 Modal energy spectrum

We have also reproduced the bifurcation line for Pm $= 1$ in Fig. 1 with the nonlinear spectral code described in more detail by Gellert, Rüdiger & Fournier (2007). For the given Lundquist number S $= 110$ both the Rm critical for ins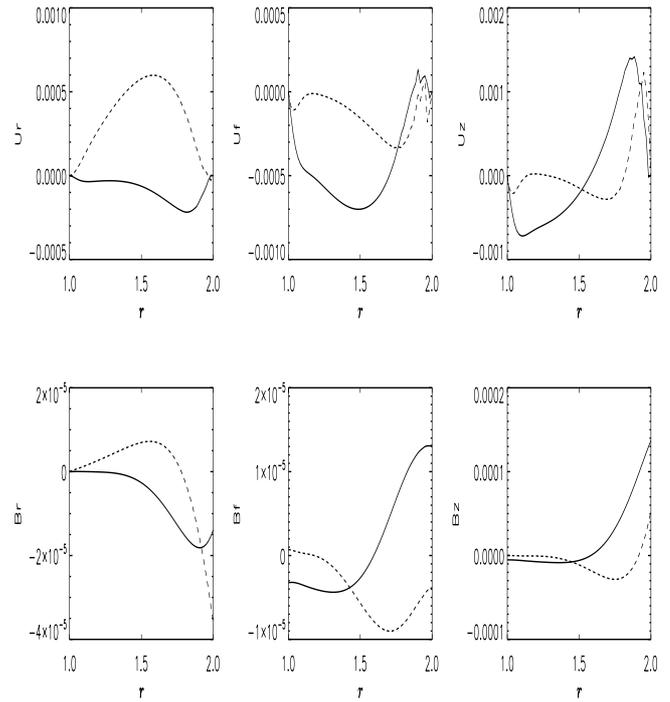tability have been identified. Here we are interested in the spectral distribution of the total magnetic energy of the instability for various azimuthal mode numbers m. The linear instability only produces a mode with $m = 1$. The smallest and the highest Reynolds number in Fig. 4 are located within the instability strip close to its boundaries. Indeed, almost all energy is concentrated at $m = 1$. In this plot the distribution of the magnetic energy of the entire volume in the modes with $m = 0, 1, 2, 3, ...$ is given. Note that the resulting energy of the axisymmetric mode ($m = 0$) exceeds the energy in the higher modes ($m \geq 2$). Hence, the nonlinearity tends to produce an inverse cascade: the magnetic energy starts from the injection mode at $m = 1$ to lower modes rather than to higher modes. Again, this is a consequence of the differential rotation which always favours axisymmetric magnetic fields on costs of the nonaxisymmetric magnetic modes. In the center of the instability strip (here at Re $= 280$, middle plot) the energies of the modes with $m = 0$ and $m = 1$ are even almost equal and only a rather small part remains for $m = 2$. Probably, the $m = 0$ energy cannot exceed, however, the energy in the $m = 1$ mode.

One can also speculate whether the series of calculations represented in Fig. 4 suggests the appearance of 'oblique rotators' such as observed in Ap stars. As Landstreet & Mathys (2000) pointed out the nonaxisymmetric part of the Ap star magnetism dominates for fast rotators and becomes basically smaller for slow rotators. This situation does *not*
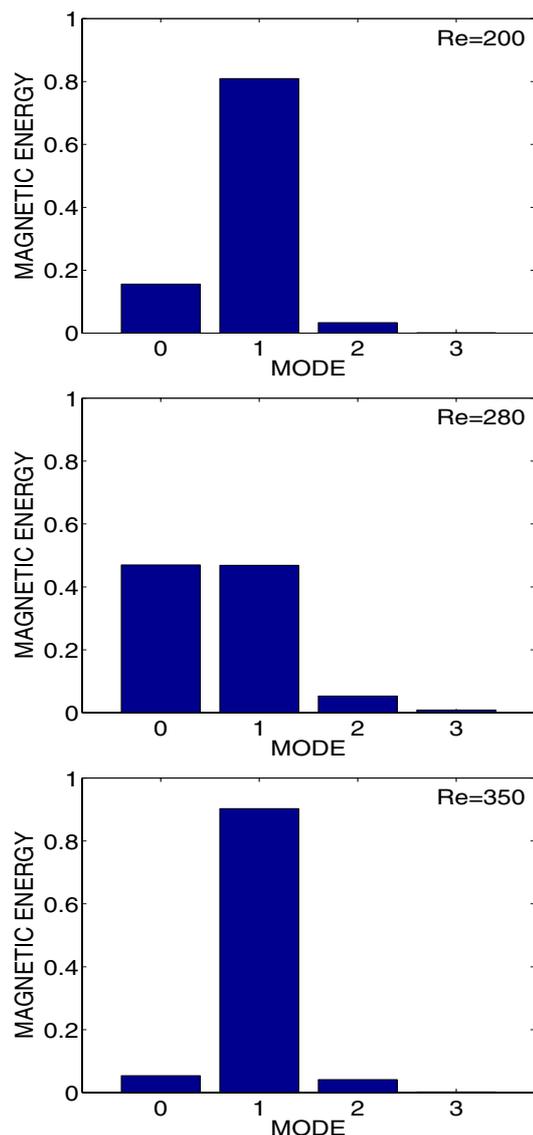
Fig. 4 (online colour at: www.an-journal.org) The magnetic energy spectrum (entire volume) of AMRI for fixed $S = 110$ and $Pm = 1$ in dependence of the Reynolds number. The plot for $Re = 280$ (*middle*) describes the high-developed instability while the plots at top and bottom more belong to the marginal instability cases.

comply with the energy spectra given in Fig. 4 – if the observed magnetic fields in Ap stars are the poloidal ones.

4 Discussion

We have shown that even if the externally imposed magnetic field is purely toroidal, one still obtains an MRI, simply non-axisymmetric rather than axisymmetric. In other respects though this new instability is remarkably like the classical axisymmetric MRI with a purely axial field, indeed far more like it than the axisymmetric MRI with a mixed field, which yielded fundamentally different scalings. In contrast, the parameters here continue to be Rm and S, just as in the classical MRI.

Note though that attempting to obtain this nonaxisymmetric MRI in a laboratory experiment would be even more difficult than attempting to obtain the classical axisymmetric MRI in an axial field. First, the required rotation rates would be even greater, $Re \gtrsim O(10^8)$, with all the difficulties that entails (Hollerbach & Fournier 2004). Even more daunting, imposing an azimuthal field of the required strength, $Ha \approx O(10^5)$, would require a current along the central axis in excess of 10^6 A, surely far beyond any feasible experiment.

This new nonaxisymmetric azimuthal MRI could have astrophysical applications though, since many astrophysical objects do have predominantly azimuthal fields, in which case the results presented here suggest that this nonaxisymmetric MRI could be preferred over the axisymmetric MRI.

Finally, one might ask how the results presented here change if one allows for a more general toroidal field profile, $B_\phi = c_1 R^{-1} + c_2 R$, where the term $c_2 R$ corresponds to an electric current flowing through the fluid itself, and not just along the central axis. Equation (7) then contains an additional term $Ha^2 rot\, \boldsymbol{B}_0 \times \boldsymbol{b}$, which opens up the possibility of instabilities driven entirely by the current $rot\, \boldsymbol{B}_0$, without any rotation necessarily present at all (Vandakurov 1972; Tayler 1973). Understanding how these current driven instabilities (also $m = 1$) interact with the magnetically catalyzed but ultimately rotationally driven MRI presented here is also in progress (see Rüdiger et al. 2007).

References

Balbus, S.A., Hawley, J.F.: 1991, ApJ 376, 214
Broderick, A.E., Narayan, R.: 2007, astro-ph/0702128
Gellert, M., Rüdiger, G., Fournier, A.: 2007, AN 328, 1162
Hollerbach, R., Fournier, A.: 2004, in: R. Rosner, G. Rüdiger, A. Bonanno (eds.), *MHD Couette Flows: Experiments and Models*, AIPC 733, p. 114
Hollerbach, R., Rüdiger, G.: 2005, PhRvL 95, 124501
Ji, H.T., Goodman, J., Kageyama, A.: 2001, MNRAS 325, L1
Landstreet, J.D., Mathys, G.: 2000, A&A 359, 213
Ogilvie, G.I., Pringle, J.E.: 1996, MNRAS 279, 152
Rüdiger, G., Zhang, Y.: 2001, A&A 378, 302
Rüdiger, G., Hollerbach, R., Schultz, M., Shalybkov, D.A.: 2005, AN 326, 409
Rüdiger, G., Hollerbach, R., Stefani, F., Gundrum, T., Gerbeth, G., Rosner, R.: 2006, ApJ 649, L145
Rüdiger, G., Hollerbach, R., Schultz, M., Elstner, D.: 2007, MNRAS 377, 1481
Stefani, F., Gundrum, T., Gerbeth, G., Rüdiger, G., Schultz, M., Szklarski, J., Hollerbach, R.: 2006, PhRvL 97, 184502, astro-ph/0606473
Tayler, R.J.: 1973, MNRAS 161, 365
Vandakurov, Yu.V.: 1972, SvA 16, 265
Velikhov, E.P.: 1959, SJETP 36, 995